Journal of Controlled Release 208 (2015) 52–58

Contents lists available at ScienceDirect

Journal of Controlled Release

journal homepage: www.elsevier.com/locate/jconrel

Doxorubicin-conjugated polypeptide nanoparticles inhibit metastasis in two murine models of carcinoma

Eric M. Mastria [a,1], Mingnan Chen [a,1,2], Jonathan R. McDaniel [a,3], Xinghai Li [a], Jinho Hyun [b], Mark W. Dewhirst [a,c], Ashutosh Chilkoti [a,d,*]

[a] Department of Biomedical Engineering, Duke University, Durham, NC 27708, United States
[b] Department of Biosystems and Biomaterials Science and Engineering, Seoul National University, Seoul 151-742, Republic of Korea
[c] Department of Radiation Oncology, Duke University Medical Center, Durham, NC 27708, United States
[d] Center for Biologically Inspired Materials and Materials Systems, Duke University, Durham, NC 27708, United States

ARTICLE INFO

Article history:
Received 28 October 2014
Received in revised form 19 January 2015
Accepted 27 January 2015
Available online 28 January 2015

Keywords:
Nanoparticle
Cancer
Metastasis
Delivery vehicle
Doxorubicin
Recombinant polypeptide

ABSTRACT

Drug delivery vehicles are often assessed for their ability to control primary tumor growth, but the outcome of cancer treatment depends on controlling or inhibiting metastasis. Therefore, we studied the efficacy of our genetically encoded polypeptide nanoparticle for doxorubicin delivery (CP-Dox) in the syngeneic metastatic murine models 4T1 and Lewis lung carcinoma. We found that our nanoparticle formulation increased the half-life, maximum tolerated dose, and tumor accumulation of doxorubicin. When drug treatment was combined with primary tumor resection, greater than 60% of the mice were cured in both the 4T1 and Lewis lung carcinoma models compared to 20% treated with free drug. Mechanistic studies suggest that metastasis inhibition and survival increase were achieved by preventing the dissemination of viable tumor cells from the primary tumor.

1. Introduction

Engineered drug delivery vehicles for cancer treatment seek to improve the clinical efficacy of chemotherapeutics by increasing the amount of drug deposited in the tumor while decreasing its accumulation in healthy tissues [1–4]. This is necessary because chemotherapeutics are commonly comprised of small hydrophobic molecules that have short plasma half-lives leading to poor bioavailability after systemic administration [5]. Sequestration of drugs into the hydrophobic core of a soluble nanocarrier has been shown to enhance the solubility and bioavailability of the drug, improve its biodistribution by preventing rapid renal clearance due to low molecular weight, and stabilize the active form of the drug within the plasma environment [6–8]. Furthermore, nanocarriers ranging between 20 and 100 nm are ideally suited to both extravasate through the leaky vasculature characteristic of rapid and uncontrolled tumor growth and accumulate within the extracellular matrix due to impaired lymphatic drainage, two pathophysiological features of tumors collectively referred to as the enhanced permeability and retention (EPR) effect [9,10].

These attractive features of drug-loaded nanoparticles led us to develop a class of recombinant chimeric polypeptide (CP) nanoparticles for the delivery of chemotherapeutics to solid tumors [1,11]. CPs are comprised of two components: (1) a hydrophilic elastin-like polypeptide (ELP) domain consisting of repeats of the pentapeptide Val-Pro-Gly-Xaa-Gly, where Xaa is any amino acid except Pro, and (2) a C-terminal $C(GGC)_7$ peptide segment that provides eight unique cysteine residues that can be used as sites for drug attachment. Conjugation of 4–6 copies of the chemotherapeutic doxorubicin (Dox) to the C-terminal drug attachment domain through an acid-labile linker results in the spontaneous self-assembly of ~40 nm diameter spherical micelles within which the drug is sequestered. We have previously demonstrated the efficacy of these CP-Dox nanoparticles in the C26 murine colon carcinoma model where ~90% of a tumor-bearing cohort was cured following a single injection [1]. While the efficacy of CP-Dox against primary tumors is encouraging, the greatest clinical need is for drugs that interfere with the metastatic cascade, as metastasis accounts for the vast majority of cancer deaths [12].

Therefore, we examine herein the overall and metastasis-free survival rate for mice bearing two syngeneic metastatic tumors, mammary 4T1 carcinoma (4T1) and Lewis lung carcinoma (LLC) engineered to

* Corresponding author at: 136 Hudson Hall, PO Box 90281, Department of Biomedical Engineering, Duke University, Durham, NC 27708-028, United States.
E-mail address: chilkoti@duke.edu (A. Chilkoti).
[1] Authors contributed equally to this work.
[2] Present affiliation: Department of Pharmaceutics and Pharmaceutical Chemistry, University of Utah, Salt Lake City, UT 84112, United States.
[3] Present affiliation: Department of Chemical Engineering, Institute for Molecular and Cellular Biology, University of Texas at Austin, Austin, TX 78712, United States.

http://dx.doi.org/10.1016/j.jconrel.2015.01.033
0168-3659/

express firefly luciferase to enable *in vivo* tracking of metastasis. Furthermore, we used a clinically relevant treatment model in which the mice were treated with a combination of chemotherapy and surgical removal of the primary tumor, enabling us to directly correlate mortality with metastatic disease.

2. Methods

2.1. Cell culture

4T1-luciferase murine mammary carcinoma cells were provided by Prof. Mark Dewhirst at Duke University Medical Center (cells certified pathogen free on 6/26/13 by IMPACT Profile III). Lewis lung carcinoma LL/2-Luc-M38 (LLC) cells were purchased from Caliper Life Sciences (certified pathogen free on 1/21/2011), after which the cells were passaged for less than 5 generations before use in animal experiments. Both cell lines were grown in DMEM supplemented with 10% FBS and cultured at 37 °C in a humidified 5% CO_2 environment.

2.2. Cytotoxicity assays

4T1 and LLC cells were seeded (10^4 cells per well) in a 96-well plate and grown for 24 h, after which they were exposed to CP-Dox or free Dox (0–100 μM equivalents) for 24 h. Cell viability was determined based on their ability to reduce tetrazolium dye (MTT assay; Promega, Madison, WI). Viability was normalized to untreated controls, and the concentration required to achieve 50% inhibition of signal (IC_{50}) was calculated.

2.3. CP-Dox synthesis

2.3.1. Synthesis and expression of chimeric polypeptides

The gene encoding the CP was synthesized from custom oligomers purchased from IDT Inc. by recursive directional ligation, as described previously [1]. The gene was cloned into a pET25b + expression vector (Novagen, Madison, WI) and transformed into BL21 (DE3) *Escherichia coli* cells (EdgeBio, Gaithersburg, MD). Transformed cells were used to inoculate 50 mL flasks supplemented with 100 μg/mL ampicillin and grown overnight at 37 °C and 190 rpm. Each 50 mL flask was used to inoculate six 1 L cultures of Terrific Broth (MOBIO, Carlsbad, CA) supplemented with ampicillin (100 μg/mL), which were grown overnight in a shaker incubator at 37 °C and 190 rpm. Protein expression was induced 5 h following inoculation by the addition of IPTG to a final concentration of 0.5 mM. Purification of the CP was carried out by inverse transition cycling (ITC), as described previously [13].

2.3.2. Conjugation of Dox to the CP

Dox was conjugated to the CP as described previously [1]. Briefly, Dox was activated by conjugation to n-ß-maleimidopropionic acid hydrazide (BMPH, Pierce Biotechnology, Rockford, IL) *via* an acid-labile hydrazone bond by stirring for 16 h in methanol supplemented with 0.1% (v/v) TFA. Separately, the purified CP was dialyzed overnight in deionized water and then reduced for 30 min in 20 mM tris carboxyethyl phosphine hydrochloride, pH 7.4 (TCEP, Pierce Biotechnology, Rockford, IL). The CP phase transition was triggered by the addition of 2.8 M NaCl, and the CP was concentrated by centrifugation (14,000 rpm for 10 min at 30 °C), after which the CP pellet was re-solubilized in 100 mM phosphate buffer (pH 7, without saline). The activated Dox-BMPH conjugate dissolved in methanol was then added dropwise to the phosphate buffer and CP solution. The final ratio of methanol to PB was 2:1. After 3 h, TCEP was added to a final concentration of 30 mM to ensure the availability of free cysteine residues for maleimide bond formation. The reaction was then left to stir overnight. The reaction solution was centrifuged using 10K MWCO Amicon centrifugal ultrafilters (Millipore, Billerica, MA) and washed with a 30% acetonitrile and 70% PBS solution for multiple cycles at 2000 rpm for 45 min to solubilize and remove unconjugated Dox-BMPH until the sample was >98% pure by gel-filtration HPLC. Finally the buffer was exchanged with PBS with additional centrifugal ultrafiltration, and endotoxin was removed by passing the CP-Dox solution through a bed of Detoxi-gel™ resin (Pierce Biotechnology, Rockford, IL). The solution was sterilized by filtration (0.2 μm pore size, VWR, Radnor, PA) and concentrated by another centrifugal ultrafiltration step (Amicon 10K MWCO, 2000 rpm, 60 min). The topographical atomic force microscopic (AFM) images were collected in tapping mode using silicon nitride cantilevers (DNP-S, Bruker, 0.35 N/m nominal spring constant; 65 kHz nominal resonant frequency) with Multimode (Bruker, Santa Barbara, USA) in liquid. AFM images were obtained at a resolution of 512 × 512 pixels using 1 Hz scan rates.

2.4. Animal studies

All animal experiments were performed in accordance with protocols approved by the Duke Institutional Animal Care and Use Committee (IACUC). BALB/c mice (Charles River, 6–10 weeks old) were inoculated with 8×10^5 4T1-luciferase cells in the 4th mammary fat pad. Albino BL6 mice (Charles River, 6–10 weeks old) were shaved and inoculated subcutaneously on the flank with 1×10^6 LLC-luc cells. Mice were treated on day 8 (post-inoculation) with free Dox or CP-Dox at the maximum tolerated dose (5 mg/kg and 20 mg/kg, respectively). Mice were sacrificed if they appeared moribund or lost more than 15% of their baseline body weight, or if the tumor volumes exceeded 2000 mm^3.

2.5. Pharmacokinetics and biodistribution

Mice were inoculated with 4T1 and treated with free Dox (5 mg/kg) or CP-Dox (20 mg/kg) on day 8 as described above. At 2, 24, 28, and 72 h after treatment, mice were sacrificed and blood and tissue samples (tumor, liver, lung, heart, spleen, kidney and paw) were obtained, processed, and analyzed for doxorubicin content by fluorescence as described previously [1]. Briefly, samples were homogenized and treated with acidified isopropanol to extract the doxorubicin, and the fluorescence of the doxorubicin in the supernatant was quantified using 485 nm for excitation and 590 nm for emission. Background fluorescence was subtracted according to calibration curves made for each organ. Drug concentration in tissues was calculated as percent of the total injected dose per gram of tissue, using calibration curves made from serial dilutions of known standards.

2.6. Primary tumor regression study (4T1)

Mice were treated on day 8 and day 15 post-inoculation with free Dox or CP-Dox at their maximum tolerated dose (MTD, 5 mg/kg and 20 mg/kg, respectively), or an equivalent volume of PBS [1]. Tumor dimensions (length and width) were measured every other day, and tumor volumes were calculated using the formula Volume (mm^3) = (length ∗ $width^2$) / 2. Groups contained 5–8 mice.

2.7. Metastasis inhibition studies

Mice were inoculated with either 4T1-luc or LLC-luc, as described above (10–12 mice per treatment group). On day 8 post-inoculation, mice were treated with free Dox (5 mg/kg) or CP-Dox (20 mg/kg). On day 15, mice were anesthetized and tumors were surgically resected. On day 22, mice were again treated with free Dox or CP-Dox at the MTD. Mice were monitored for metastasis and primary tumor recurrence 2×/week using the IVIS Xenogen bioluminescent imaging system (Caliper LS, Hopkinton, MA). Mice were sacrificed after observing a detectable metastatic signal in two consecutive imaging sessions, or if the mice became moribund (>15% weight loss or the presence of hyperventilation). The presence of metastases that were detected *via* bioluminescence was later confirmed by post-mortem dissection.

2.8. Statistical analysis

Statistical analyses were performed using JMP Statistical Software and GraphPad Prism. Multiple groups were compared using ANOVA followed by Tukey–Kramer (Tukey's HSD) test where applicable. Event-time plots were made using Kaplan–Meier technique and analyzed using the log-rank test. Unless otherwise noted, error bars are +/− standard error of the mean.

3. Results and discussion

3.1. CP-Dox micelles demonstrate improved pharmacokinetics and biodistribution compared to free drug

Upon conjugation to doxorubicin, individual CP chains self-assemble into approximately 40 nm diameter micelles, as visualized by AFM, which we term CP-Dox (Fig. 1a). The AFM results are consistent with previously reported dynamic light scattering (DLS) data where CP-Dox was found to have a hydrodynamic radius (Rh) of 21.5 nm [1]. CP-Dox maintains the ability to achieve maximal cytotoxicity when applied to 4T1 mammary carcinoma cells *in vitro*, exhibiting a slight increase in the IC_{50} relative to freely dissolved doxorubicin (0.46 μM and 2.0 μM for free Dox and CP-Dox, respectively, Fig. 1b). This effect, which is commonly observed for polymer–drug conjugates, is attributable to an impaired ability for the drug to diffuse across the cell membrane when attached to a hydrophilic carrier [5].

Despite this slight decrease in efficacy *in vitro*, we anticipated that this nano-carrier would vastly improve the *in vivo* efficacy of the drug by increasing the maximum tolerated dose, lengthening the plasma half-life, and improving the biodistribution compared to that of the free drug. The maximum tolerated dose (MTD), as determined by the largest IV bolus dose that did not cause greater than 15% body weight loss, increased from 5 mg/kg for free Dox to 20 mg/kg for CP-Dox in both BALB/c (Fig. 2d) and Albino BL/6 mice (data not shown).

We next examined the pharmacokinetics and biodistribution of doxorubicin, where free Dox and CP-Dox were injected at their respective MTDs. As shown in Fig. 1c, the plasma level of free doxorubicin was essentially undetectable as early as 2 h post-injection, which is consistent with the short half-life of doxorubicin (~5 min) in mice [14]. In contrast, conjugating doxorubicin to the CP greatly extended the plasma residence time of Dox as well as increased the concentration within the plasma compartment, with low but detectable levels remaining even 72 h following treatment. The elimination half-life of doxorubicin, when delivered as CP-Dox, is increased to 11.0 h, and the plasma clearance is 0.271 mL/h. The intratumoral accumulation of free Dox was poor, with less than 1% of the injected dose per gram of tumor tissue (%ID/g) detectable in the tumor at 2 h, and undetectable drug levels at 24 h (Fig. 1d). On the other hand, CP-Dox displayed 5% ID/g of tumor tissue 24 h post-injection. Remarkably, CP-Dox treated tumors retained significantly more doxorubicin after 72 h than the free Dox treated tumors retained only 2 h following administration ($p < 0.05$, t-test).

On the basis of the %ID/g, the liver, kidney and paw were targeted to a greater extent by CP-Dox than free Dox. We examined the paw

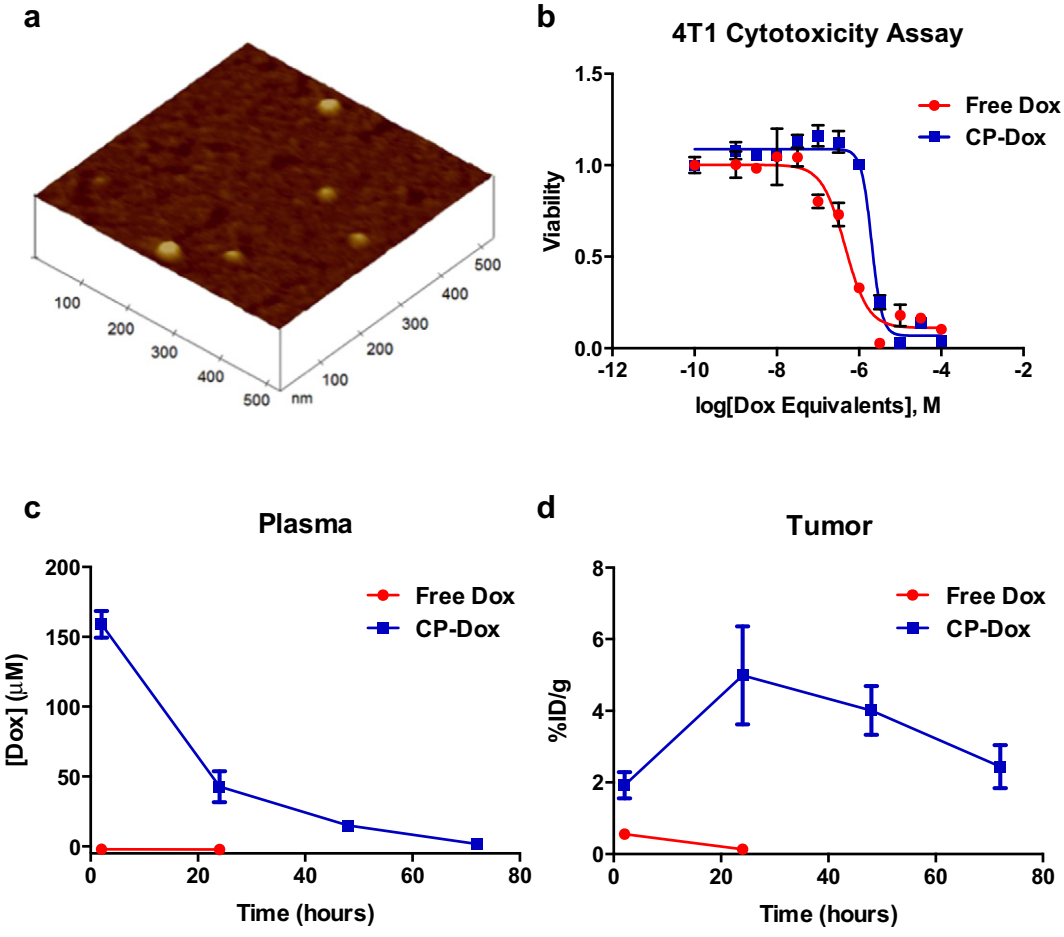

Fig. 1. (a) Tapping mode atomic force microscopy (AFM) image of CP-Dox nanoparticles on mica in phosphate buffered saline (PBS). CP-Dox micelles have a diameter of approximately 40 nm. (b) *In vitro* cytotoxicity assay of free Dox and CP-Dox against 4T1 mammary carcinoma. IC_{50} values were 2.0 μM and 0.46 μM for CP-Dox and free Dox, respectively. (c) After intravenous bolus administration of free Dox (5 mg/kg) and CP-Dox (20 mg/kg) to BALB/c mice, CP-Dox extends the half-life of doxorubicin to 11.0 h, with a corresponding clearance of 0.271 mL/h (n = 3 mice/group). (d) CP-Dox improves the tumor accumulation compared to free doxorubicin in an orthotopic 4T1 mammary carcinoma model (n = 3 mice/group).

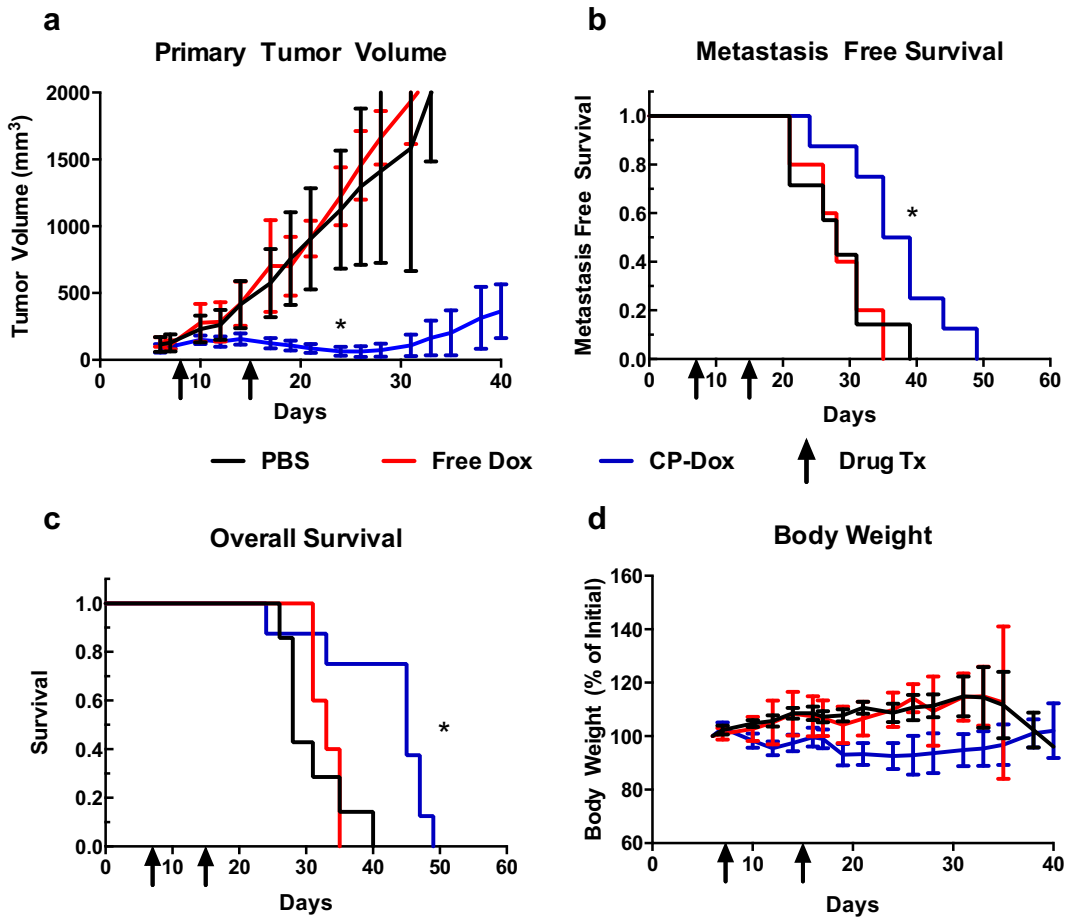

Fig. 2. 4T1 cells were implanted on day 0 and mice were treated with CP-Dox, free Dox, or a vehicle control on days 8 and 15. (a) Primary tumor volume was significantly lower in CP-Dox compared to free Dox and PBS groups ($p < 0.05$, ANOVA). (b) Metastasis-free survival and (c) overall survival were significantly improved by CP-Dox treatment ($p < 0.05$, log-rank). (d) Percent of initial body weight as a function of days post-tumor inoculation. Note: Error bars in (a) and (d) are 95% confidence interval, n = 5–8/group. The black arrows (labeled Drug Tx in the legend) show the days on which the animals were treated with either PBS, free Dox or CP-Dox nanoparticles.

because of the propensity for doxorubicin nanoparticles to cause hand–foot syndrome, wherein the drug leaks into the capillaries of the hands and feet, causing pain and redness [15]. The low level of the drug (<1% ID/g) in this tissue is therefore reassuring. Concentrations of Dox in the heart, spleen, and lungs were similar for CP-Dox and free doxorubicin (Supplementary Fig. S1).

3.2. CP-Dox prolongs survival and delays metastasis in an orthotopic murine mammary carcinoma model

To investigate the effect of the improved pharmacokinetics and biodistribution on therapeutic efficacy, BALB/c mice were inoculated with 8×10^5 tumor cells in the 4th mammary fat pad, and were then treated with CP-Dox or free Dox at their respective maximum tolerated doses on days 8 and 15 post-inoculation. 4T1-luc is a highly metastatic murine mammary tumor that metastasizes to the lungs, liver, and brain [16], and responds poorly to free Dox treatment *in vivo* [17,18]. Mammary fat pad inoculation was used because orthotopic tumors are known to more aggressively metastasize and be more refractory to chemotherapy than *s.c.* tumors [19,20]. For these reasons, the 4T1 model presents many of the challenges faced in the clinic by chemotherapeutics.

Fig. 2a illustrates that CP-Dox significantly inhibited primary tumor growth ($p < 0.05$, ANOVA). Furthermore, treatment delayed the development of metastasis (Fig. 2b), which resulted in improved overall survival of the mice when compared to a no-treatment control (PBS) or free Dox (Fig. 2c, $p < 0.05$, log-rank). Mouse body weights were followed as a surrogate marker for the toxicity of the drug treatments. This treatment schedule (2 treatments separated by 1 week) was well tolerated, with no mice losing more than 15% of their original body weight, as shown in Fig. 2d. Two treatments demonstrated markedly reduced metastasis when compared to a single dose (8 days post-inoculation; Supplementary Fig. S2b). No further improvement in primary tumor or metastasis inhibition was observed with three doses (Supplementary Fig. S2d).

3.3. CP-Dox enhances survival in two metastatic murine tumor models when combined with primary tumor resection

We next instituted a treatment regimen that consisted of chemotherapy a week before surgery (neoadjuvant; day 8), followed by surgical resection of the primary tumor (day 15) and chemotherapy a week after surgery (adjuvant; day 22). We included surgical resection because it allowed us to isolate the effect of the primary tumor burden from metastatic disease in causing mortality. This treatment regimen also allowed us to test CP-Dox in a more clinically relevant scenario, which is significant to its translation to the clinic.

We found that surgical removal of the 4T1 mammary carcinoma was successful in achieving local control of disease, as no mice developed local recurrence in either treatment group. Furthermore, as seen in Fig. 3a, the combination of CP-Dox and surgery greatly improved the therapeutic outcome over free Dox with surgery ($p < 0.05$, log-rank) and stand-alone CP-Dox treatment without surgery (Fig. 3b). In fact, over half of the CP-Dox treated mice survived to the end of the 80 day study, which in our experience is a sufficient length of time to ensure

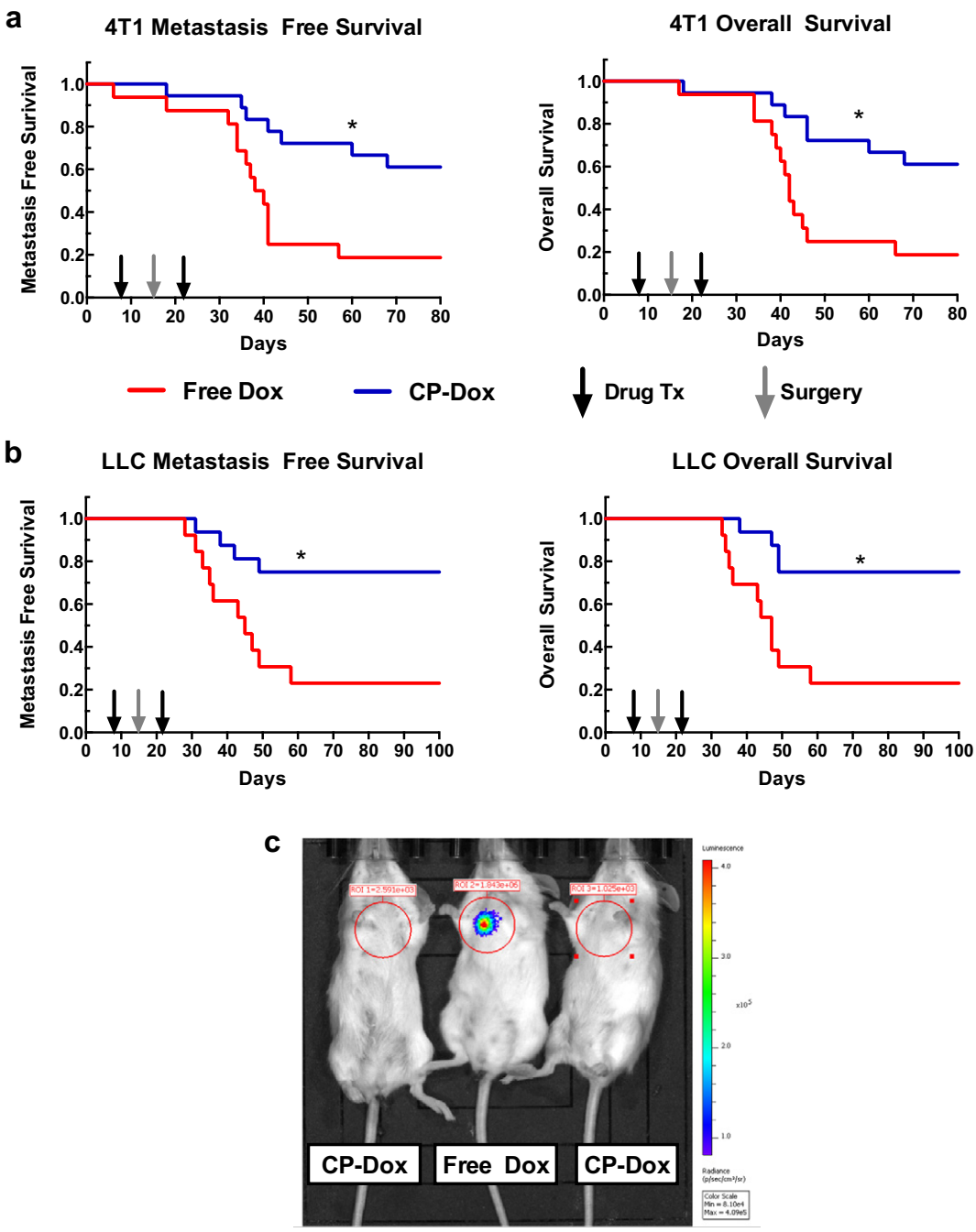

Fig. 3. Neoadjuvant and adjuvant treatment by CP-Dox significantly prolongs metastasis-free and overall survival in both the (a) 4T1 and (b) LLC metastatic tumor models in a surgical resection model ($p < 0.05$, log-rank). (c) *In vivo* luciferase imaging of BALB/c mice bearing orthotopic 4T1-luc tumors. A free Dox treated mouse (middle) shows lung metastases, while the CP-Dox treated mice (left and right) are metastasis free at day 35. Note: n = 10–12/group. Black arrows = drug treatment (free Dox or CP-Dox). Gray arrows = primary tumor resection.

a long-term cure for this tumor model. For the free Dox cohort, only 20% of the mice achieved a long-term cure. Fig. 3c shows a bioluminescent image from day 35, at which point the orthotopic 4T1 primary tumor has been surgically removed. The mouse treated with free Dox (middle) has developed a detectable lung metastasis, while the mice treated with CP-Dox (left and right), remain metastasis free.

To further demonstrate the ability of CP-Dox to inhibit metastasis, we used the same treatment regimen for subcutaneously implanted Lewis lung carcinoma engineered to express luciferase. Similar to 4T1, it is a syngeneic cell line that is widely used to study metastasis in immune-competent mice, and it responds poorly to free Dox *in vivo*, despite exhibiting sensitivity to the drug *in vitro* (Supplementary Fig. S3) [21,22]. For this model, 1×10^6 cells were inoculated into the flank of BL6 Albino mice on day 0, followed by CP-Dox or free Dox neoadjuvant treatment on day 8, primary tumor resection on day 15, and adjuvant chemotherapy on day 22. The LLC cells were more locally invasive than the 4T1 cells, leading to a significant number of mice exhibiting local primary tumor recurrence. The incidence of this primary tumor recurrence was, however, highly asymmetric, with only 7% of the CP-Dox cohort experiencing tumor recurrence compared to 46% of the free Dox cohort ($p < 0.05$, Fisher's Exact), despite identical surgical techniques for both groups. Metastasis-free survival and overall survival

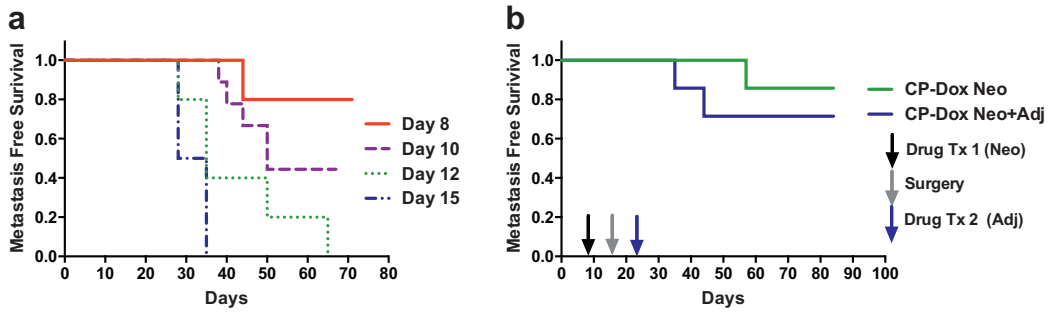

Fig. 4. CP-Dox inhibits metastasis by delaying dissemination of metastasis forming cells from the primary tumor. (a) Effect of surgical resection day on survival, demonstrating that in untreated mice, metastasis forming cells spread from the primary tumor between day 8 and day 12 for the majority of mice. (b) Effect of adjuvant treatment with CP-Dox on metastasis free survival, demonstrating that the adjuvant CP-Dox treatment confers no survival benefit beyond that seen for neo-adjuvant CP-Dox ($p > 0.05$, log-rank). The black arrow in panel (b) represents the neoadjuvant treatment received by both cohorts of mice. The gray arrow denotes the day of surgery, while the blue arrow represents the adjuvant treatment, only received by the CP-Dox Neo + Adj group.

were significantly prolonged in the CP-Dox group (Fig. 3b; $p < 0.05$, log-rank).

3.4. CP-Dox inhibits metastasis by delaying dissemination of viable cells from the primary tumor

Our results clearly demonstrate the ability of CP-Dox to inhibit metastasis in two cell lines, so we next explored the question of which step of the metastatic process was interrupted by our treatment. The metastatic cascade involves multiple steps, including invasion from the primary tumor into the blood stream, travel through the circulatory system, arrest in a distant organ, and finally growth into a metastasis [23]. To elucidate the timing of these steps in the 4T1 model, we removed primary tumors on Days 8, 10, 12, or 15 and then observed the metastasis-free survival of mice. As shown in Fig. 4a, only about 20% of the mice develop metastases if the primary tumor is removed on day 8 or earlier, whereas all mice that received surgery on day 12 or day 15 succumbed to metastasis. This means that for the majority of mice, cells with the potential to form metastases spread from the primary tumor between day 8 and day 12.

As most mice do not contain viable micrometastases on the day of Dox treatment (day 8), we hypothesized that the survival benefit of CP-Dox stems largely from the neoadjuvant treatment preventing the dissemination of viable cells from the primary tumor rather than by exerting a direct cytotoxic effect on micrometastases. To test this hypothesis, we repeated the 4T1 chemotherapy and resection experiments described above, but included a cohort that only received the neoadjuvant treatment (CP-Dox Neo). As shown in Fig. 4b, withholding adjuvant treatment had no discernible effect on survival with these sample sizes ($p > 0.05$, log-rank, $n = 7$ in each group). Furthermore, adjuvant therapy alone with CP-Dox after surgery on day 12 conferred no survival advantage compared to free Dox or PBS (data not shown). Taken together, these experiments strongly suggest that with the time points used for chemotherapy and resection in this study, neoadjuvant treatment by CP-Dox inhibits metastasis by preventing the dissemination of viable cells from the primary tumor to distant organs. This result is perhaps not surprising since CP-Dox was designed to take advantage of leaky vasculature and improve accumulation in the primary tumor. Micrometastases, the putative target of adjuvant treatment, may be relatively avascular and therefore difficult to target with macromolecular carriers [24,25].

4. Conclusion

We have shown that CP-Dox inhibits metastasis and improves the survival of mice in two syngeneic metastatic cell lines. Our study is particularly relevant to clinical translation because 90% of cancer deaths in patients are caused by metastasis [12] rather than the growth of the primary tumor. Our treatment approach of chemotherapy and surgical tumor resection expands the scope of a typical drug delivery study that only follows primary tumor growth. This focus on primary tumor growth by the field of drug delivery may be a contributing factor to the relatively slow adoption of new delivery systems in the clinic [24]. Indeed, our drug delivery vehicle succeeded in enhancing doxorubicin's accumulation in the primary tumor, and while our results demonstrate a strong inhibition of metastasis, our data suggest that the effect arises from improved control of the dissemination of invasive cells from the primary tumor. Nonetheless, the ability to prevent metastasis by controlling the primary tumor is clinically important in the setting of neoadjuvant treatments administered to downstage a tumor and enable surgery [26]. During the treatment, it is critical that the cells are not able to spread from the primary tumor. Our results suggest that our drug formulation would be a more effective neoadjuvant agent compared to freely dissolved drug.

Supplementary data to this article can be found online at http://dx.doi.org/10.1016/j.jconrel.2015.01.033.

Disclosure of potential conflicts of interest

A.C. has a financial interest in PhaseBio Pharmaceuticals, which has licensed the ELP technology from Duke University.

Acknowledgments

This research was supported by grant awarded to A.C. from the National Institutes of Health (R01 EB000188). E.M. acknowledges support from the Medical Scientist Training Program Grant (T32 GM007171). The authors thank Leon Cai for his preparation of the graphical abstract.

References

[1] J. MacKay, M. Chen, J. McDaniel, W. Liu, A. Simnick, A. Chilkoti, Self-assembling chimeric polypeptide–doxorubicin conjugate nanoparticles that abolish tumours after a single injection, Nat. Mater. 8 (2009) 993–999. http://dx.doi.org/10.1038/nmat2569.
[2] D. Peer, J. Karp, S. Hong, O. Farokhzad, R. Margalit, R. Langer, Nanocarriers as an emerging platform for cancer therapy, Nat. Nanotechnol. 2 (2007) 751–760. http://dx.doi.org/10.1038/nnano.2007.387.
[3] M. Davis, Z. Chen, D. Shin, Nanoparticle therapeutics: an emerging treatment modality for cancer, Nat. Rev. Drug Discov. 7 (2008) 771–782. http://dx.doi.org/10.1038/nrd2614.
[4] N. Kamaly, Z. Xiao, P. Valencia, A. Radovic-Moreno, O. Farokhzad, Targeted polymeric therapeutic nanoparticles: design, development and clinical translation, Chem. Soc. Rev. 41 (2012) 2971–3010. http://dx.doi.org/10.1039/c2cs15344k.
[5] R. Duncan, Polymer conjugates as anticancer nanomedicines, Nat. Rev. Cancer 6 (2006) 688–701. http://dx.doi.org/10.1038/nrc1958.
[6] S.R. Croy, G.S. Kwon, Polymeric micelles for drug delivery, Curr. Pharm. Des 12 (2006) 4669–4684.
[7] P. Brusa, M.L. Immordino, F. Rocco, L. Cattel, Antitumor activity and pharmacokinetics of liposomes containing lipophilic gemcitabine prodrugs, Anticancer Res. 27 (2007) 195–199 (published online 2007/03/14).

[8] J. Fassberg, V.J. Stella, A kinetic and mechanistic study of the hydrolysis of camptothecin and some analogues, J. Pharm. Sci. 81 (1992) 676–684. http://dx.doi.org/10.1002/jps.2600810718 (published online 1992/07/01).
[9] H. Maeda, J. Wu, T. Sawa, Y. Matsumura, K. Hori, Tumor vascular permeability and the EPR effect in macromolecular therapeutics: a review, J. Control. Release 65 (2000) 271–284. http://dx.doi.org/10.1016/S0168-3659(99)00248-5.
[10] R. Duncan, The dawning era of polymer therapeutics, Nat. Rev. Drug Discov. 2 (2003) 347–360. http://dx.doi.org/10.1038/nrd1088.
[11] J.R. McDaniel, S.R. MacEwan, M. Dewhirst, A. Chilkoti, Doxorubicin-conjugated chimeric polypeptide nanoparticles that respond to mild hyperthermia, J. Control. Release 159 (2012) 362–367. http://dx.doi.org/10.1016/j.jconrel.2012.02.030.
[12] P. Mehlen, A. Puisieux, Metastasis: a question of life or death, Nat. Rev. Cancer 6 (2006) 449–458. http://dx.doi.org/10.1038/nrc1886.
[13] D. Meyer, A. Chilkoti, Purification of recombinant proteins by fusion with thermally-responsive polypeptides, Nat. Biotechnol. 17 (1999) 1112–1115. http://dx.doi.org/10.1038/15100.
[14] A. Gabizon, D. Tzemach, L. Mak, M. Bronstein, A.T. Horowitz, Dose dependency of pharmacokinetics and therapeutic efficacy of pegylated liposomal doxorubicin (DOXIL) in murine models, J. Drug Target. 10 (2002) 539–548. http://dx.doi.org/10.1080/1061186021000072447 published online 2003/04/10.
[15] D. Lorusso, A. Di Stefano, V. Carone, A. Fagotti, S. Pisconti, G. Scambia, Pegylated liposomal doxorubicin-related palmar-plantar erythrodysesthesia ('hand–foot' syndrome), Ann. Oncol. 18 (2007) 1159–1164.
[16] B. Pulaski, S. Ostrand-Rosenberg, Mouse 4T1 breast tumor model, in: John E. Coligan, et al., (Eds.)Current Protocols in Immunology, 2001 http://dx.doi.org/10.1002/0471142735.im2002s39 (Chapter 20).
[17] Z.-G. Gao, L. Tian, J. Hu, I.-S. Park, Y. Bae, Prevention of metastasis in a 4T1 murine breast cancer model by doxorubicin carried by folate conjugated pH sensitive polymeric micelles, J. Control. Release 152 (2011) 84–89. http://dx.doi.org/10.1016/j.jconrel.2011.01.021.
[18] Y. Yang, D. Pan, K. Luo, L. Li, Z. Gu, Biodegradable and amphiphilic block copolymer–doxorubicin conjugate as polymeric nanoscale drug delivery vehicle for breast cancer therapy, Biomaterials (2013) http://dx.doi.org/10.1016/j.biomaterials.2013.07.037.
[19] Z. Dong, R. Radinsky, D. Fan, R. Tsan, C. Bucana, C. Wilmanns, I. Fidler, Organ-specific modulation of steady-state mdr gene expression and drug resistance in murine colon cancer cells, J. Natl. Cancer Inst. 86 (1994) 913–920. http://dx.doi.org/10.1093/jnci/86.12.913.
[20] M. Bibby, Orthotopic models of cancer for preclinical drug evaluation: advantages and disadvantages, Eur. J. Cancer 40 (2004) 852–857. http://dx.doi.org/10.1016/j.ejca.2003.11.021.
[21] Y. Yoshimoto, M. Kawada, D. Ikeda, M. Ishizuka, Involvement of doxorubicin-induced Fas expression in the antitumor effect of doxorubicin on Lewis lung carcinoma in vivo, Int. Immunopharmacol. 5 (2005) 281–288. http://dx.doi.org/10.1016/j.intimp.2004.09.032.
[22] Y. Jia, M. Yuan, H. Yuan, X. Huang, X. Sui, X. Cui, F. Tang, J. Peng, J. Chen, S. Lu, W. Xu, L. Zhang, Q. Guo, Co-encapsulation of magnetic Fe_3O_4 nanoparticles and doxorubicin into biodegradable PLGA nanocarriers for intratumoral drug delivery, Int. J. Nanomedicine 7 (2012) 1697–1708. http://dx.doi.org/10.2147/ijn.s28629.
[23] J. Joyce, J. Pollard, Microenvironmental regulation of metastasis, Nat. Rev. Cancer 9 (2009) 239–252. http://dx.doi.org/10.1038/nrc2618.
[24] T. Lammers, F. Kiessling, W.E. Hennink, G. Storm, Drug targeting to tumors: principles, pitfalls and (pre-) clinical progress, J. Control. Release 161 (2012) 175–187. http://dx.doi.org/10.1016/j.jconrel.2011.09.063.
[25] A. Schroeder, D.A. Heller, M.M. Winslow, J.E. Dahlman, G.W. Pratt, R. Langer, T. Jacks, D.G. Anderson, Treating metastatic cancer with nanotechnology, Nat. Rev. Cancer 12 (2012) 39–50. http://dx.doi.org/10.1038/nrc3180.
[26] H.M. Kuerer, L.A. Newman, T.L. Smith, F.C. Ames, K.K. Hunt, K. Dhingra, R.L. Theriault, G. Singh, S.M. Binkley, N. Sneige, T.A. Buchholz, M.I. Ross, M.D. McNeese, A.U. Buzdar, G.N. Hortobagyi, S.E. Singletary, Clinical course of breast cancer patients with complete pathologic primary tumor and axillary lymph node response to doxorubicin-based neoadjuvant chemotherapy, J. Clin. Oncol. 17 (1999) 460–469.